Theory of Fast Walking With Human-Driven Load-Carrying Robot Exoskeletons

Tiange Zhang and David J. Braun

***Abstract*— Reaching and maintaining high walking speeds is challenging for a human when carrying extra weight, such as walking with a heavy backpack. Robotic limbs can support a heavy backpack when standing still, but accelerating a backpack within a couple of steps to race-walking speeds requires limb force and energy beyond natural human ability. Here, we conceive a human-driven robot exoskeleton that could accelerate a heavy backpack faster and maintain top speeds higher than what the human alone can when not carrying a backpack. The key components of the exoskeleton are the mechanically adaptive but energetically passive spring limbs. We show that by optimally adapting the stiffness of the limbs, the robot can achieve near-horizontal center of mass motion to emulate the load-bearing mechanics of the bicycle. We find that such an exoskeleton could enable the human to accelerate one extra body weight up to top race-walking speeds in ten steps. Our finding predicts that human-driven mechanically adaptive robot exoskeletons could extend human weight-bearing and fast-walking ability without using external energy.**

***Index Terms*— Exoskeletons, variable stiffness spring legs, mechanically adaptive robots.**

I. Introduction

HUMANS have attempted to increase their fast-walking and load-bearing capability for centuries. Using head-support, African women are able to carry 70% of their body-weight up to 1.7-meter-per-second walking speed [1]–[3], while using forehead straps, Nepalese porters can carry up to 200% of their body weight [4], [5] at the same speeds.

Backpacks are the most conventional ways of carrying a load [6], although walking with a heavy backpack is exhausting. Supporting a backpack is energetically demanding, partly because muscles require energy to produce force even if they do not do mechanical work [7]–[9] – standing requires more than 1-watt-per-kilogram extra power [10]. Energy is also required to accelerate and decelerate a backpack – 7-watts-per-kilogram when walking at normal speeds (1.25-meter-per-second) [11]. Finally, energy is required to compensate for collision energy losses as the foot strikes the ground [8], [12], [13]. As a result, the top speed of walking with a backpack is lower than the top speed of walking without a backpack.

One way to reduce the energy needed to carry a load is to use wheels. Wheels can eliminate the collision energy loss in legged motion and reduce the acceleration as well as deceleration of the load compared to legs [12]. Furthermore, the bicycle allows a world-class cyclist to generate 19 watt-per-kilogram average power [14], enough to accelerate one extra body weight from rest to the top race-walking speeds (4 meter-per-second) in less than 1 second. However, translating the benefits of wheeled mechanics to legged locomotion has been a fundamental challenge [15].

Prior theoretical studies of legged locomotion have investigated the means to emulate the benefits of wheels by increasing leg swing frequency and decreasing step length [13], [15]. These studies have found that the benefits of wheeled transportation can be achieved in legged locomotion at the limit of infinitely small step lengths. Instead of taking small steps, a spring can be used to obtain some beneficial aspects of wheeled motion. A spring placed in parallel with the leg can support a heavy load [16], [17]. A spring placed in series with the leg can reduce collision energy loss. A spring may also enable the human to supply energy, such as, allowing the human to compress the spring when the leg is in the air. These benefits could theoretically enable humans to jump twice as high with jumping stilts compared to athletic shoes, and have led to a new theory of jumping and running using variable stiffness spring limbs [18], [19].

In this paper, we present the theory of a mechanically adaptive robot exoskeleton, enabling fast acceleration and efficient walking at race-walking speeds while carrying up to one extra body weight. The exoskeleton is a human-powered robot that resembles an elliptical exercise machine (Fig. 1). The key component of the exoskeleton is the mechanically adaptive and energetically passive spring leg, which can be compressed by the human lower limb during both swing and stance, similar to a human riding a bicycle.

Using a point mass leg model of the exoskeleton (Section II), we ask the following two questions: (i) How can we optimally adapt the leg stiffness in a fast walking load-carrying task? (ii) What limits the top speed, the number

Manuscript received 5 February 2022; revised 18 May 2022; accepted 9 June 2022. Date of publication 14 July 2022; date of current version 22 July 2022. This work was supported in part by a Seeding Success Grant provided by Vanderbilt University and the National Science Foundation CAREER Award under Grant No. 2144551. *(Corresponding author: David J. Braun.)*

The authors are with the Advanced Robotics and Control Laboratory, Center for Rehabilitation Engineering and Assistive Technology, Department of Mechanical Engineering, Vanderbilt University, Nashville, TN 37235 USA (e-mail: tiange.zhang@vanderbilt.edu; david.braun@vanderbilt.edu).

Digital Object Identifier 10.1109/TNSRE.2022.3190208

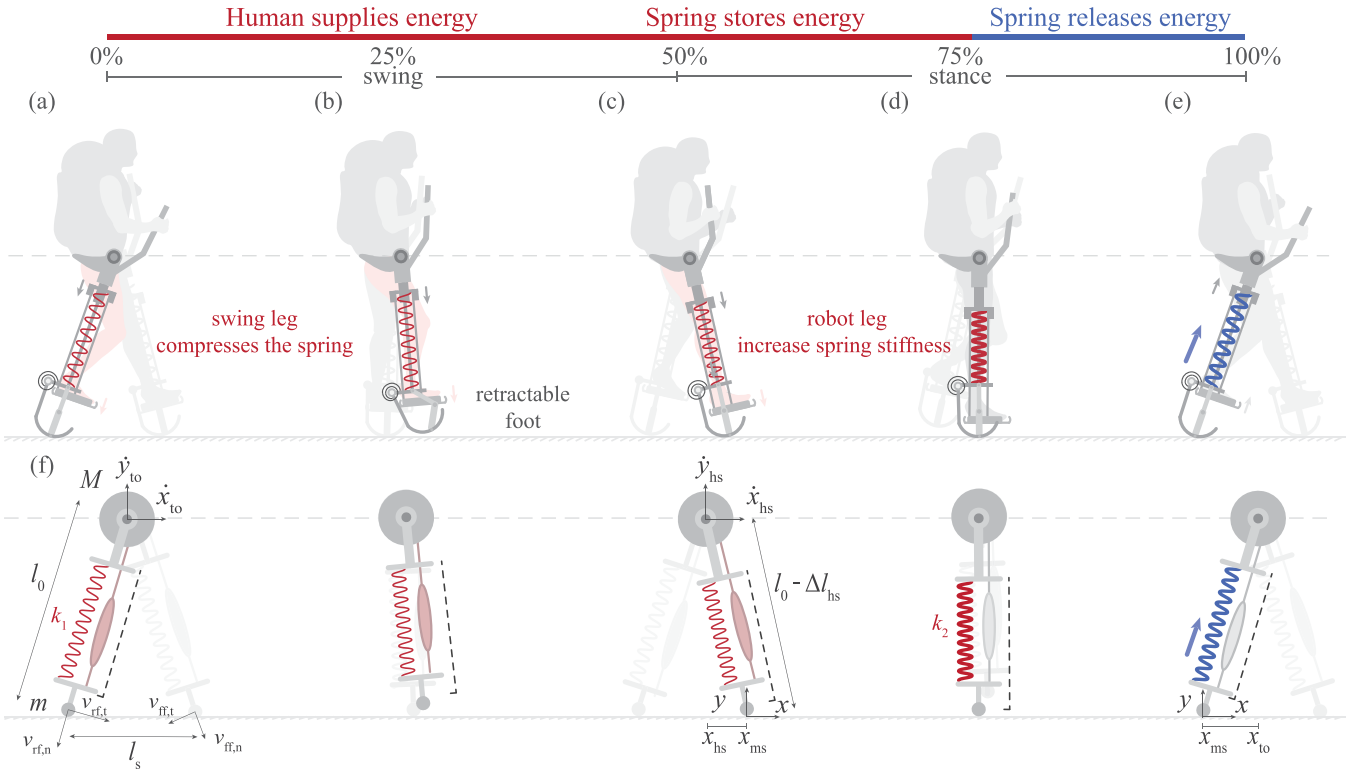

Fig. 1. Working principle of the human-driven load-bearing exoskeleton. During swing (a-c), the human leg compresses the spring, while the arms pulling on the handle bars facilitate leg rotation. Also, during the swing (a-c), the foot of the robot is retracted by a small torsional spring to provide ground clearance. As the swing leg touches the ground (c), the weight of the human and the extra load from the backpack further compress the spring leg until mid-stance. At mid-stance (d), the stiffness of the spring leg increases from k_1 to k_2. From mid-stance and toe-off (d-e), the energy stored by the spring is released. In the model of the human-driven robot, the human uses a "sliding pedal". The sliding pedal allows the human to independently move the foot up and down (to compress the spring) and rotate the robot leg (to take a step). The point-mass spring-leg model of the exoskeleton is shown in (f). The hard stop (black dashed lines) prevents the robot leg to overextend.

of steps to reach the top speed, and the maximum amount of payload that can be carried by a robot solely driven by human power? We address the first question by deriving the optimal feedback relation between the leg stiffness and the step length (Section III) which enables fast acceleration and energy efficient steady-state locomotion at top race-walking speeds (Section IV). We address the second question by establishing the theoretical limits of the top speed, the number of steps to reach the top speed, and the payload that can be carried by the exoskeleton (Section V).

We predict that a human-powered robot exoskeleton – that has variable stiffness spring legs, but no actuators to provide energy beyond what is supplied by the human [20]–[22] – can address two fundamental physical limitations of carrying extra weight at high walking speeds: (i) the energy bottleneck of accelerating rapidly and (ii) the efficiency bottleneck of maintaining top race-walking speeds at low energy cost. We further show that the maximum weight that can be carried by the human at top race-walking speeds is set by the leg swing frequency, the energy supplied by the human per step, and the stiffness of the robot leg, instead of the strength of the human leg (Section V).

In summary, we find that human-powered robot exoskeletons could change the physical demand imposed on the human body when carrying heavy loads. In particular, the proposed conceptual robot exoskeleton could enable the human to use smaller leg force supplied continuously during a step, as opposed to a higher leg force supplied over a short period at the end of each step, to carry a heavy load (Fig. 1). The exoskeleton is therefore similar to the bicycle which enables cyclists with weaker legs but better endurance to move faster than sprinters with strong and powerful legs. We envision that human-powered robot exoskeletons may benefit emergency rescue, sports, recreation, and transportation, as the legged alternative to the bicycle.

II. Mathematical Model

The exoskeleton is a mechanically adaptive and energetically passive robot which has variable stiffness spring legs (Fig. 1). In order to move the exoskeleton, the human leg supplies energy by compressing the spring leg (Fig. 1a-d). Part of the energy is supplied by the human pushing the pedal attached to the foot downwards during the swing phase (Fig. 1a-c) while the rest of the energy is supplied by compressing the spring by the weight of the human and the backpack from heel-strike to mid-stance (Fig. 1c-d). At mid-stance, the stiffness of the spring is changed such that all the energy supplied by the human until mid-stance is released from mid-stance to toe-off (Fig. 1d-e). During late stance, as the spring extends and returns to its

uncompressed length, the human leg retracts to its initial bent position (Fig. 1a).

While the human body has more than two hundred degrees of freedom and over six hundred muscles, the center of mass motion of the human-driven robot can be studied using simple models. Here, we use one of the simplest point-mass spring-leg models to study human-driven robot locomotion (Fig. 1), previously used to study human and robot locomotion [23].

A. Model of the Robot

For the human-driven robot, the equations governing the planar motion of the center of mass are given by:

$$M\ddot{x} = F(x,y)\frac{x}{l(x,y)} \quad \text{and} \quad M\ddot{y} = F(x,y)\frac{y}{l(x,y)} - Mg, \tag{1}$$

where (x, y) define the position of the center of mass with respect to the coordinate system fixed to the foot at heel-strike, M is the mass of the human and the backpack, g is the gravitational acceleration, $l = l(x, y) = \sqrt{x^2 + y^2}$ is the leg length, while $F(x, y)$ is the force of the robot leg.

In our model, the force of the robot leg is provided by a linear spring with natural length l_0, stiffness k_1 before mid-stance, and stiffness k_2 after mid-stance (Fig. 1f):

$$F(x,y) \in \begin{cases} k_1\big(l_0 - l(x,y)\big) & \text{if} \quad x < 0 \\ k_2\big(l_0 - l(x,y)\big) & \text{if} \quad x \geq 0. \end{cases} \tag{2}$$

The change of stiffness at mid-stance from k_1 to k_2 in (2) is a result of the parallel coupling of two springs – the leg spring of stiffness k_1 compressed to l_{ms} from heel-strike to mid-stance, and an auxiliary spring of stiffness $k_2 - k_1$ pre-compressed by Δl_{ms} from toe-off to mid-stance. Because the coupling of the two springs at mid-stance resembles a variable stiffness spring that instantaneously changes stiffness from k_1 to k_2, we represent the two springs in the robot leg with one variable stiffness spring in (2) and Fig. 1. The challenges of designing a variable stiffness spring will be discussed in Section VI.

The energy that drives the robot is the energy supplied by the human from toe-off to mid-stance (Fig. 1a-d). This is the energy released by the variable stiffness spring from mid-stance to toe-off (Fig. 1d-e):

$$\Delta E = \frac{1}{2}k_1\Delta l_{\text{hs}}^2 + \frac{1}{2}(k_2 - k_1)\Delta l_{\text{ms}}^2, \tag{3}$$

where Δl_{hs} denotes the spring deformation at heel-strike, and Δl_{ms} denotes the spring deformation at mid-stance. We will consider the collision energy loss due to the foot ground contact, as a dominant form of energy loss in legged locomotion [15]. We estimate the collision loss by assuming instantaneous double support and ideal plastic impact:

$$\Delta E_{\text{loss}} \approx \frac{1}{2}mv_{\text{ff}}^2 + \frac{1}{2}M\left(\frac{J}{J + l_0^2 M}\right)v_{\text{ff,t}}^2 + \frac{1}{2}mv_{\text{ff,n}}^2, \tag{4}$$

where v_{ff} is the absolute velocity of the front foot just before heel-strike, $v_{\text{rf,n}}$ is the relative velocity of the rear foot with respect to the center of mass in the direction of the leg just before take-off, while $v_{\text{ff,t}}$ is the absolute tangential velocity of the front foot just before heel-strike (Fig. 1f). The first term in (4) is due to the foot mass at heel-strike [24], the second term comes from the non-negligible leg inertia [25], while the third term is due to the hard stop (dashed lines in Fig. 1f) that prevents the rear leg from over-extending [19].

Finally, we assume that the robot is $\eta \times 100\%$ efficient. In particular, we consider a robot that can supply no more energy ΔE than what is supplied by the human per step ΔE_h:

$$\eta = \frac{\Delta E}{\Delta E_h} \in [0, 1]. \tag{5}$$

We note that a 95% efficient robot exoskeleton ($\eta = 0.95$) is similar to a modern bicycle [14] while a 50% efficient robot exoskeleton ($\eta = 0.5$) is similar to an early bicycle [26].

B. Robot Driven by the Human

The motion of the robot will depend on the motion of the human (Fig. 1a-e). In particular, we assume that the human can (i) take smaller or longer steps to control the step length of the robot l_s, (ii) swing the legs slower or faster to control the step frequency of the robot f, and (iii) supply more or less energy ΔE_h by compressing the leg spring, to control the amount of energy that can be used to move the robot. The step length, step frequency, and the amount of energy supplied by the human per step, are subject to biological limitations:

$$0 \leq l_{\text{s}} \leq l_{\text{s max}}, \quad 0 \leq f \leq f_{\text{max}}, \quad 0 \leq \Delta E_h \leq \Delta E_{h\,\text{max}}. \tag{6}$$

In both human and robot locomotion, larger hip angle results in larger step length for the same leg length. We assume that the maximal hip angle of the robot is the same as the maximal hip angle of a race-walking athlete when walking at top race-walking speeds. Consequently, the maximal dimensionless step length s_{max} is larger than one, such that the maximal step length is 20% larger than one leg length [27]:

$$s_{\text{max}} = \frac{l_{\text{s max}}}{l_0} = \frac{6}{5}. \tag{7}$$

Adding extra mass to the human leg reduces the step frequency if the same hip torque is used [28], [29]. Consequently, we assume that the swing frequency of the robot leg f is limited by the maximum swing frequency of the un-augmented human leg $f_{\text{max}} = 3.35\ Hz$ [27]. Reaching the maximum human leg frequency may be possible if the hip torque is amplified by the arms shown in Fig. 1, a torsional hip spring as discussed in [30], or using the combination of both.

The maximum amount of energy a robot leg can supply per step depends on the energy generation rate of the human legs and the time available for the human to supply energy. The average energy generation rate of a world-class cyclist is $\dot{E}_{\text{h max}}/m_{\text{body}} \approx 19$ W/kg [14] where m_{body} is the body mass. The time available for the human legs to supply energy depends on the design of the robot leg. For example, if the design only allows the human leg to supply energy when the robot leg touches the ground, then the human leg will be able to supply energy 25% of the stride time (from heel-strike to mid-stance, Fig. 1c-d). On the other hand, if the design allows

the human leg to supply energy in the air, then the human leg will be able to supply energy 75% of the stride time (from toe-off to mid-stance, Fig. 1a-d). In both cases, the energy generated by one human leg during a stride can be released by one robot leg during a step. Consequently, assuming that the robot exoskeleton allows the human to supply the same amount of energy as the bicycle, the maximal amount of energy that can be supplied by the human legs per stride (and released by an ideal 100% efficient robot legs per step) is:

$$e_{\mathrm{h\,max}} = \frac{\Delta E_{\mathrm{h\,max}}}{m_{\mathrm{body}}} = \frac{3}{2}\frac{\dot{E}_{\mathrm{h\,max}}}{f m_{\mathrm{body}}} \tag{8}$$

where the factor of $3/2$ implies that no more than 75% of the stride time is available for each human leg to supply energy.

In order to obtain the most conservative estimate for the maximal amount of energy that can be supplied during a stride $e_{\mathrm{h\,max}}$, we assume $f = f_{\max}$ in (8), and obtain $e_{\mathrm{h\,max}} \approx 8$ J/kg for a world-class cyclist. Consequently, the energy that can be provided by a human per stride is:

$$e_{\mathrm{h}} \in [0, 8] \text{ J/kg}. \tag{9}$$

The range of energies per stride includes non-world-class cyclists as well as average humans [31].

III. Optimal Fast Walking With a Heavy Load

The average top speed of walking cannot exceed the speed defined by the maximal step frequency and the maximal step length:

$$\bar{\dot{x}} \leq \bar{\dot{x}}_{\max} = l_{\mathrm{s\,max}} f_{\max}. \tag{10}$$

However, reaching the top speed defined by the maximal step frequency and maximal step length is nontrivial, as it requires a special walking technique, one that circumvents walk-to-run transition at speeds lower than the top speed. In order to define one such technique, we take inspiration from cycling, where the wheels keep the center of mass on a straight line. Keeping the center of mass on a straight line prevents take-off at any speeds, but it does not define how to control the robot limb to rapidly accelerate and efficiently walk at the top speed.

In Section III-A, we define the walking motion where the center of mass moves close to a straight line. In Section III-B, we formulate an optimization problem to define the adaptation of the spring leg to rapidly reach top race-walking speeds.

A. Reducing Vertical Oscillations

The principle of work and energy implies that the total change of the kinetic and potential energy of the center of mass from heel-strike to toe-off must be equal to the energy supplied and the energy dissipated during each step:

$$E_{\mathrm{to}} - E_{\mathrm{hs}} = \Delta E_{\mathrm{x}} + \Delta E_{\mathrm{y}} = \Delta E - \Delta E_{\mathrm{loss}}. \tag{11}$$

According to this relation, maximizing the change of the energy in the horizontal direction ΔE_{x} – as required to rapidly accelerate the center of mass – is equivalent to minimizing the change of the energy in the vertical direction:

$$\begin{aligned}(y^*_{\mathrm{to}}, \dot{y}^*_{\mathrm{to}}) &= \operatorname{argmin}_{(y,\dot{y})\in\mathscr{Y}} \Delta E_{\mathrm{y}}(y, \dot{y}) \\ \mathscr{Y} &= \left\{(y, \dot{y}) \in \mathbb{R}^2 : y_{\min} \leq y \leq l_0, -\epsilon \leq \dot{y} \leq \epsilon\right\}\end{aligned} \tag{12}$$

where $\Delta E_{\mathrm{y}}(y, \dot{y}) = \frac{1}{2}M(\dot{y}^2 - \dot{y}^2_{\mathrm{hs}}) + Mg(y - y_{\mathrm{hs}})$ is the total mechanical energy in the vertical direction, y_{hs} and y_{to} are the vertical positions of the center of mass at heel-strike and toe-off, $\mathscr{Y}$ contains the feasible vertical positions and velocities of the center of mass, $y_{\min} \geq 0$ is the minimal vertical distance of the center of mass measured from the ground surface, while ϵ is an arbitrarily small non-negative number.

The solution of (12) is $(y^*_{\mathrm{to}}, \dot{y}^*_{\mathrm{to}}) = (y_{\min}, 0)$. This solution is consistent with steady-state walking where the energy released by the spring per step is the same as the energy dissipated $\Delta E - \Delta E_{\mathrm{loss}} = 0$, while the velocity at heel-strike and toe-off do not change $\Delta E_{\mathrm{x}} = 0$; therefore, $\Delta E_{\mathrm{y}} = 0$. Relation $\Delta E_{\mathrm{y}} = 0$, together with the periodicity of the trajectory and the periodicity of the vertical center of mass velocity implies:

$$y^*_{\mathrm{hs}} = y^*_{\mathrm{to}} = y_{\min} \quad \text{and} \quad \dot{y}^*_{\mathrm{hs}} = \dot{y}^*_{\mathrm{to}} = 0. \tag{13}$$

Conditions (13) satisfy the straight-line motion of the center of mass in cycling at any speed – $\forall t \in \mathbb{R}_+ : y(t) = y_{\min}$, $\dot{y}(t) = 0$. In the remainder of this paper, we will use these conditions to define the walking technique of the conceptual human-powered robot shown in Fig. 1.

B. Speeding up as Fast as Possible

Minimizing the energy in the vertical direction (12) promotes a straight-line center of mass motion, but it does not define how much energy is used in each step. Smaller amounts of energy may be used to speed up slowly, while more energy may be required to speed up rapidly, but what is the fastest way to reach the top speed while the center of mass moves along a trajectory consistent with (13)?

The following optimization problem defines the compression of the leg before heel-strike Δl_{hs}, the stiffness of the leg before heel-strike k_1, and the stiffness of the leg at mid-stance k_2, to achieve the largest increase in velocity per step subject to all previously mentioned constraints:

$$\begin{aligned}(\Delta l^*_{\mathrm{hs}}, k^*_1, k^*_2) &= \operatorname{argmax}_{(\Delta l_{\mathrm{hs}}, k_1, k_2)\in\mathscr{D}_3} \Delta E(\Delta l_{\mathrm{hs}}, k_1, k_2) \\ \mathscr{D}_3 &= \left\{(\Delta l_{\mathrm{hs}}, k_1, k_2) \in \mathbb{R}^3 : (1), (2), (6), (13)\right\},\end{aligned} \tag{14}$$

where ΔE is the energy stored by the robot leg (3), while $\mathscr{D}_3$ contains the governing equations (1) and (2), the constraint that limits the step frequency, step length, the amount of energy that can be provided by the human (6), and the condition that facilitates a particular (near-straight line) center of mass motion (13).

IV. The Optimal Control Program

We aim to derive the optimal feedback relation between the leg-length at heel-strike, the stiffness of the leg during early stance, and the stiffness of the leg during late stance.

The optimization problem (14) can be solved numerically (see Fig. 2). However, the numerical solution can only provide limited insight into the relation between the physical parameters (mass, leg length, step length, and gravity) and the optimal leg compression and stiffness. Such relation could inform the

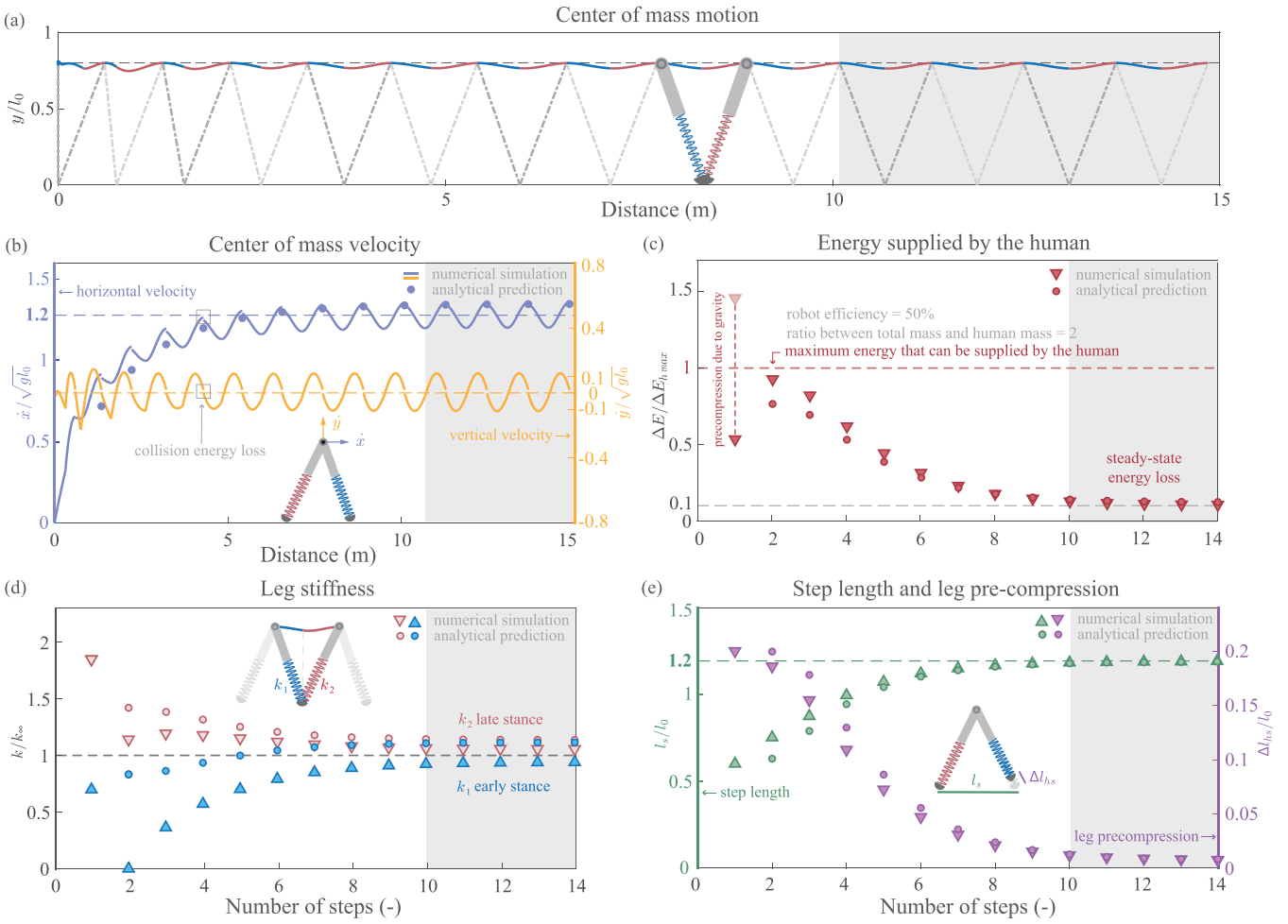

Fig. 2. Numerical simulation results and the corresponding analytical predictions of loaded fast walking. In all figures, the lines and triangles (△ ▽) represent the numerical results while the circles (○) represent the corresponding analytical predictions. (a) Trajectory of the center of mass and the orientation of the legs during stance. The gray dashed lines represent the alternating stance legs. (b) Velocity in the forward horizontal and the upward-downward vertical directions. (c) Energy required per step normalized by the maximal amount of energy that can be generated by a human. (d) Normalized stiffness of the robot leg before mid-stance k_1 and after mid-stance k_2. The normalization is done using the steady-state stiffness. (e) Step length l_s and leg pre-compression Δl_{hs}.

design and control of human-driven robots, and enable us to establish the physical performance limits of human-driven walking robots.

Although it is not possible to derive an exact analytically solution of (14), it is possible to derive an approximate solution of (14), under the following simplified assumptions: (i) the horizontal motion of the center of mass is approximated by $\forall t \in \mathbb{R}_+ : y(t) \approx y_{\min}$ near the top walking speed $\bar{\dot{x}} \approx \bar{\dot{x}}_{\max} = l_{s\max} f_{\max}$, (ii) the leg mass is negligible compared to the combined mass of the body and the extra load $m/M \ll 1$, and (iii) the moment of inertia of the leg is negligible compared to the moment of inertia of the center of mass with respect to the foot touching the ground $J/Ml_0^2 \ll 1$. The effect of these assumptions will be evaluated in Section IV-E.

A. Compression of the Spring Leg at Heel-Strike

For any walking motion, the compression of the spring leg at heel-strike Δl_{hs} is limited by the maximal step length $s_{\max}$, defined in (7):

$$0 \le \frac{\Delta l_{\text{hs}}}{l_0} \le \frac{\Delta l_{\text{hs}\max}}{l_0} \le 1 - \sqrt{1 - \frac{1}{4} s_{\max}^2}, \tag{15}$$

while for the optimal walking with the maximal leg swing frequency $f = f_{\max}$, the maximal compression of the spring leg depends on the actual and the maximal forward speed at heel-strike (see Section VI-A):

$$\frac{\Delta l_{\text{hs}\max}}{l_0} \approx 1 - \sqrt{1 - \left(\frac{1}{4} - \left[\frac{\dot{x}_{\text{hs}}}{\dot{x}_{\text{hs}\max}} - \frac{1}{2}\right]^2\right) s_{\max}^2}. \tag{16}$$

Based on (15) and (16), we predict that the leg approaches its uncompressed length at the top speed:

$$\bar{\dot{x}} = \bar{\dot{x}}_{\max} \Rightarrow l_{\text{s}} = l_{\text{s}\max} \Rightarrow \Delta l_{\text{hs}\max} \approx 0. \tag{17}$$

In Section IV-D, we will use the maximal leg compression at heel-strike and the forward speed (16) to define the optimal leg compression and the optimal step length in each step.

B. Spring Stiffness Before and After Mid-Stance

For the optimal walking, there is an approximate linear relation between the spring stiffness before mid-stance k_1 and after mid-stance k_2 to ensure zero vertical velocity at heel-strike and toe-off $\dot{y}_{\text{hs}} = \dot{y}_{\text{to}} = 0$ (see Section VI-B):

$$k_2 \approx 2\, k_\infty - k_1, \tag{18}$$

where

$$\frac{k_\infty l_0}{Mg} \approx \frac{2s_{\max}}{\sqrt{4-s_{\max}^2}\left(\ln\left(\frac{2+s_{\max}}{2-s_{\max}}\right)-s_{\max}\right)} \approx 8. \quad (19)$$

According to (18), smaller leg stiffness in early stance k_1 necessitates larger leg stiffness in late stance k_2 to keep the vertical velocity zero at heel-strike and toe-off, while the average leg stiffness k_∞ (19) remains the same in every step.

In Section IV-D, we will use (18) to define the optimal leg stiffness in late-stance k_2 for each step.

C. Spring Stiffness at Heel-Strike

For the optimal walking, the step frequency is limited by how fast the human can swing their legs $f \leq f_{\max}$. This limitation provides a lower bound on the leg stiffness before mid-stance (see Section VI-C):

$$k_{1\,\min}(\Delta l_{\rm hs}) \leq k_1 \leq k_\infty, \quad (20)$$

where the minimum stiffness is

$$\frac{k_{1\,\min}(\Delta l_{\rm hs})}{k_\infty} \approx 1 - \frac{2}{s_{\max}^2\left(1-\frac{1}{2}\left(\frac{1-l^*}{(1-\frac{1}{2}\sqrt{4-s_{\max}^2})}\right)^2\right)}\frac{\Delta l_{\rm hs}}{l_0}, \quad (21)$$

and l^* denotes the dimensionless leg length when the instantaneous forward speed equals the average top forward speed.

While the implication of violating (20) may be unclear at first sight, a leg stiffness smaller than $k_{1\,\min}(\Delta l_{\rm hs})$ would lead to a swing frequency higher than the maximal swing frequency $f > f_{\max}$.

According to (18), (19), (20), and (21), the stiffness of the leg spring in early stance will approach the stiffness of the leg spring in late stance, and both will approach the steady-state stiffness at the top speed:

$$\bar{\dot{x}} = \bar{\dot{x}}_{\max} \Rightarrow k_1 \approx k_2 \approx k_\infty. \quad (22)$$

In Section IV-D, we will use (20) to define the optimal leg stiffness at early-stance k_1 in each step.

D. The Optimal Control Program

Using the linear relation between the stiffness before and after mid-stance (18), we can rewrite the energy required per step (3) into the following relation $\Delta E = \frac{1}{2}k_1\Delta l_{\rm hs}^2 + \frac{1}{2}(k_2 - k_1)(l_0 - y_{\min})^2 = k_\infty(l_0 - y_{\min})^2 - \frac{1}{2}k_1[2(l_0 - y_{\min})^2 - \Delta l_{\rm hs}^2]$. Consequently, (14) can be recast into the following minimization problem:

$$(\Delta l_{\rm hs}^*, k_1^*) \approx \operatorname{argmin}_{(\Delta l_{\rm hs}, k_1)\in\mathscr{D}_2}\left[\frac{1}{2}k_1[2(l_0 - y_{\min})^2 - \Delta l_{\rm hs}^2]\right]$$
$$\mathscr{D}_2 \approx \left\{(\Delta l_{\rm hs}, k_1) \in \mathbb{R}^2 : (15), (16), (19), (20), (21)\right\}. \quad (23)$$

The minimization problem (23), together with (18), defines the approximate analytical solution of the original optimization problem (14):

$$\Delta l_{\rm hs}^* = \Delta l_{\rm hs\,max}, \quad k_1^* = k_{1\,\min}(\Delta l_{\rm hs}^*), \quad k_2^* = k_{2\,\max}(\Delta l_{\rm hs}^*), \quad (24)$$

where $\Delta l_{\rm hs\,max}$ is defined by (16), $k_{2\,\max} = 2k_\infty - k_{1\,\min}(\Delta l_{\rm hs})$ is defined by (18), and $k_{1\,\min}(\Delta l_{\rm hs})$ is defined by (21). The approximate solution of the optimization problem (24) predicts that (i) the leg compression should be maximized at heel-strike, (ii) the stiffness of the leg should be minimized at heel-strike, while (iii) the stiffness of the leg should be maximized after mid-stance given all the physical constraints.

One way to implement the optimal control program (24) is to make the robot a human-driven automaton, a machine where the human supplies energy $\Delta E \leq \Delta E_h$ by compressing the spring leg, while the robot adjusts the leg length $\Delta l_{\rm hs}$ (consequently the step length l_s) and the spring stiffness, k_1 and k_2. Such an implementation is not contingent upon the human providing the exact amount of energy per step, since providing enough energy (not less than what is needed) is sufficient to realize the optimal control program.

Making the robot a human-driven automaton is facilitated by the approximate analytical solution of the optimization problem (24), which suggests that the spring stiffness can be parameterized by a measurable quantity, the leg compression, or equivalently, the step length. However, making the robot a human-driven automaton would not guarantee the optimal performance of the walking machine, since using the robot optimally would require the human to learn the optimal walking technique – compress the leg optimally, or choose the optimal step length according to (16). Learning a better walking technique is similar to learning a better cycling technique, or learning a better ice-skating technique, first to avoid falling, and then to move faster. Further practical aspects of human-driven walking robots are discussed in Section VI.

E. Discarding the Simplifying Assumptions

We have numerically simulated the walking motion starting from stand-still and up to the top speed, see Fig. 2. The simulation assumes one extra body weight ($M/m_{\rm body} = 2$) and considers a 50% efficient exoskeleton ($\eta = 0.5$). The simulation takes into account the feet mass (5% of the total mass), the added robot leg (making the leg inertia twice of the human leg inertia), and the collision energy loss (4).

Because of the assumptions made at the beginning of this section, we do not expect the analytical predictions to provide a good estimate of the numerical results at all speeds, but we do expect the analytical predictions to provide a reasonable estimate of the numerical predictions at high speeds. Consequently, we expect the numerical solution to complement the analytical results during the starting steps at low speeds. Next, we compare the numerical results (solid lines and triangles) with the analytical predictions (circles) presented in Fig. 2.

Figure 2a shows the center of mass trajectory as it reaches top race-walking speeds; 4 meter-per-second. We observe that the error between the simulated (solid line) and the ideal (dashed line) motion of the center of mass is less than 5%.

Figure 2b shows the horizontal and vertical speeds (light blue and orange lines). We observed that 90% of the top forward speed is reached within 5 steps, and that the top speed is reached within 10 steps. The same figure shows that the vertical velocity is zero at heel-strike and toe-off, consistent with (13), and remains close to zero during the

motion (light orange line). The same figure also shows that the analytical prediction of the forward speed (circles) overestimates the average forward speed (dashed light blue line) by less than 5%.

Figure 2c shows the energy required to accelerate the load from rest to the top speed. We observe that (i) the maximum amount of energy the human can supply (dashed red line) is more than the energy needed to carry one extra body weight using a 50% efficient exoskeleton (triangles below the dashed red line) and (ii) the energy needed during steady-state walking at the top speed is approximately 10% of the maximal amount of energy. The analytical prediction (circles) underestimates the energy required during the initial steps, and overestimates the energy required during steady-state walking (triangles). The error in the latter case is less than 2%. The error in the former case is less than 16%. Despite the error, the analytical prediction captures the decreasing trend of the energy needed per step even at the starting steps.

Figure 2d shows the stiffness of the robot leg before and after mid-stance (triangles). We observe that (i) the leg stiffness at early stance k_1 increases, (ii) the leg stiffness at late stance k_2 decreases, while (iii) the average leg stiffness approaches a constant value k_∞. The analytical prediction (circles) shows the same trend, although it slightly overestimates the numerical values. The overestimation of the steady-state stiffness (19) is less than 10% at high speeds; the error mainly comes from discarding the collision energy loss and assuming horizontal center of mass motion. At lower speeds, the analytical prediction only captures the trend in stiffness change, while at the second step, the numerical simulation predicts zero leg-stiffness, not captured by the analytical prediction. The zero leg-stiffness predicted by the numerical simulation (triangle) shows that due to the high-acceleration at the end of the first step, the center of mass "flies through" the early stance phase of the second step, where the support from the spring leg is not needed.

Figure 2e shows the step length (green) and the leg pre-compression (purple) at heel-strike. We observe that the step length increases until it reaches the maximal step length defined by (7), while the leg pre-compression decreases until it reduces to nearly zero. The analytical prediction shows the same trend. The error between the numerical simulation results (triangles) and the analytical predictions (circles) is less than 5%.

In summary, despite the complexity of the optimization problem (14), the analytical solution we derived (24) is relatively simple, provides valuable insights, and compares reasonably well with the numerical predictions, even though the numerical results are not being subject to the modeling assumptions listed at the beginning of this section.

V. Theoretical Limits

Using the analytical approximation of the optimal spring leg adaptation strategy (24), we will present a number of prediction formulas – dimensionless relations between system parameters and system performance [32] – that establish the performance limits, and facilitate the design and control of the human-powered walking robot shown in Fig. 1.

A. What Limits the Top Walking Speed?

The top speed of walking is defined by the maximal step frequency and the maximal step length (10):

$$\frac{\bar{\dot{x}}_{\max}}{\sqrt{gl_0}} = \frac{f_{\max} l_{s\max}}{\sqrt{gl_0}} = \frac{6}{5}\sqrt{\frac{l_0}{g}} f_{\max} \approx \frac{6}{5}. \tag{25}$$

However, reaching the top speed necessitates a special walking technique. The importance of the walking technique can be exemplified by compass gait walking where the center of mass moves along a circular arc [33]. The compass gait triggers the walk-to-run transition at $\bar{\dot{x}}_{\max}/\sqrt{gl_0} \leq 1$ [16], [34], which is at least 20% below the top speed of the spring leg exoskeleton (25).

B. How Many Steps Are Needed to Reach the Top Speed?

The numerical simulation suggests that it take 5 steps to reach 90% of the top speed, and 10 steps to practically reach the top speed. Furthermore, by neglecting the collision energy loss $\Delta E_{\text{loss}} = 0$, and substituting the energy per step ΔE (24), $\Delta E_y = 0$, and (3), into the energy balance (11), we obtain the following analytical relation:

$$\frac{\dot{x}_{\text{to}}^2}{gl_0} \approx \frac{\dot{x}_{\text{hs}}^2}{gl_0} + \frac{3}{2}\frac{\Delta l_{\text{hs}\max}}{l_0}, \tag{26}$$

where the maximal compression of the spring leg at heel-strike $\Delta l_{\text{hs}\max}$ (16) does not depend on the total mass M.

The above relation is the reason that the velocity plot in Fig. 2b remains the same regardless of the load carried by the robot. Relation (26) also implies that optimally accelerating a heavier backpack will require more energy.

C. Is the Optimal Walking Stable?

The recurrence relation in (26) predicts the change in the forward velocity for the next step $\dot{x}_{n+1} = \dot{x}_{\text{to}}$ based on the velocity at the current step $\dot{x}_n = \dot{x}_{\text{hs}}$. These predictions are shown with circles in Fig. 2b. To assess the stability of the walking motion, we have linearized (26) around the top speed. The linearized relation is given by $\dot{x}_{n+1} = \left(1 - \frac{3}{8}\frac{gl_0}{\dot{x}_{\text{hs}\max}^2} s_{\max}^2\right)\dot{x}_n \approx \left(1 - \frac{3}{8}\frac{g}{l_0 f_{\max}^2}\right)\dot{x}_n$. This linear recurrence relation predicts that the optimal walking is locally stable, close to the top speed, under the following condition:

$$\frac{\sqrt{3}}{4} < \sqrt{\frac{l_0}{g}} f_{\max}. \tag{27}$$

According to (27), the step frequency cannot be arbitrarily small for a given leg length, and the leg length cannot be arbitrarily small for a given step frequency. Condition (27) is consistent with the numerical simulation in Fig. 2, where $\sqrt{l_0/g}\, f_{\max} \approx 1$. Finally, we note that, this stability result pertains to the speed and is contingent upon the human moving the swing foot forward fast enough to avoid stumbling.

D. What Is the Maximum Amount of Energy Required per Step?

For the optimal walking, the energy required per step linearly depends on the mass. The following approximate

formula is obtained by substituting (26) into the energy balance (11):

$$\frac{\Delta E - \Delta E_{\text{loss}}}{Mgl_0} \approx \frac{3}{4}\frac{\Delta l_{\text{hs max}}}{l_0}. \tag{28}$$

According to (28), the maximal amount of energy is expected during the first step because $\Delta l_{\text{hs max}}/l_0$ is a monotone increasing function, see Fig. 2e. However, at the first step, the spring already stores a considerable amount of energy because it is pre-compressed by the weight of the load and the human, as shown in Fig. 2c (the energy stored by the spring is shown by the difference between the light and the dark triangles for the first step). Consequently, the human supplies the most energy during the second step, see Fig. 2c (triangle).

Using (26) and (28), and by assuming negligible collision loss at the initial steps $\Delta E_{\text{loss}} \ll \Delta E_{\text{max}}$, we estimate the maximal energy per step during optimal walking:

$$\frac{\Delta E_{\text{max}}}{Mgl_0} \approx \frac{3}{4}\left(1 - \sqrt{1 - \frac{1}{4}s_{\text{max}}^2}\right) \approx \frac{3}{20}. \tag{29}$$

This prediction underestimates the numerically computed energy at the second step by 16%.

The following condition is obtained using (8) and (29):

$$\frac{\Delta E_{\text{max}}}{\Delta E_{\text{h max}}} \approx \frac{3}{4}\left(1 - \sqrt{1 - \frac{1}{4}s_{\text{max}}^2}\right)\frac{M}{m_{\text{body}}}\frac{gl_0}{\eta e_{\text{h max}}} \leq 1. \tag{30}$$

This condition ensures that the energy needed for the optimal walking can be supplied by the human. In particular, $\Delta E_{\text{max}}/\Delta E_{\text{h max}} = 1$ provides an estimate of the horizontal dashed line in Fig. 2c. Whether the energy needed for the optimal walking is below or above the dashed line depends on the mass M/m_{body}, the efficiency of the exoskeleton η, and the energy that can be supplied by the human $e_{\text{h max}}$.

Figure 2c shows that carrying one extra body-weight $M/m_{\text{body}} \approx 2$ would necessitate a world-class cyclist $e_{\text{h max}} \approx 8$ J/kg (9) driving a 50% efficient exoskeleton $\eta = 0.5$ (5). The inequality relation (30) slightly underestimates the energy needed to carry one extra body weight $\Delta E_{\text{max}}/\Delta E_{\text{h max}} \approx 0.76$ (circle) compared to the numerical prediction $\Delta E_{\text{max}}/\Delta E_{\text{h max}} \approx 0.93$ (triangle) shown in Fig. 2c.

E. How Much Energy Is Needed to Maintain the Top Speed?

At the top speed, the minimum amount of energy required per step is the energy lost at heel-strike (4). This energy is proportional to the mass of the robot foot and the rotational inertial of the robot and the human leg:

$$\frac{\Delta E_{\text{min}}}{Mgl_0} = \frac{\Delta E_{\text{loss}}}{Mgl_0} \approx \mathcal{O}\left(\frac{m}{M}, \frac{J}{Ml_0^2}\right). \tag{31}$$

Because the spring leg decouples the mass of the backpack from the mass of the robot foot, the collision energy loss at heel-strike is not proportional to the total mass, as it would be for an exoskeleton with rigid legs. Consequently, the collision energy loss does not increase if more mass is carried by the exoskeleton. Therefore, a properly designed – at least 50% efficient, low foot mass (5% of the total weight) and low rotational inertia (same as the human leg) – spring leg exoskeleton has the capacity to carry a heavy backpack (comparable to one body weight) at top race-walking speeds, with low energy cost per step (10% of the maximum amount of energy needed to speed up the total mass), as shown in Fig 2.

F. What Limits the Total Weight?

The load that can be carried by the human-driven robot is limited by the maximum stiffness of the robot limb during optimal walking $k_{\text{max}} \approx 2\ k_\infty$, see Fig. 1d. The following inequality relation was obtained by substituting $k_{\text{max}} \approx 2\ k_\infty$ into (19):

$$\frac{Mg}{k_{\text{max}}l_0} \leq \frac{\sqrt{4 - s_{\text{max}}^2}\left(\ln\left(\frac{2+s_{\text{max}}}{2-s_{\text{max}}}\right) - s_{\text{max}}\right)}{4s_{\text{max}}} \approx \frac{1}{16}. \tag{32}$$

The energy that can be supplied by the human per leg during a stride must be more than the maximal amount of energy required to optimally move the total mass (30). This condition also places an upper bound on the total weight:

$$\frac{M}{m_{\text{body}}} \leq \frac{4}{3}\frac{1}{1 - \sqrt{1 - \frac{1}{4}s_{\text{max}}^2}}\frac{\eta e_{\text{h max}}}{gl_0} = \frac{20}{3}\frac{\eta e_{\text{h max}}}{gl_0}. \tag{33}$$

According to (33), the extra weight that can be sped up by the human to top race-walking speeds within 10 steps is limited by the maximal energy that can be supplied by the human per stride (9), instead of the maximal human leg stiffness or force.

The analytical formula (33) suggests that the optimally controlled human-sized ($l_0 \approx 1$ m) robot exoskeleton, which is only half as efficient as a modern racing bicycle ($\eta \approx 0.5$), could enable a world-class cyclist ($e_{\text{h max}} \approx 8$ J/kg) to carry one extra body-weight $M/m_{\text{body}} \approx 2$ to top race-walking speeds (4 meters-per-second), within 10 steps.

The analytical formula (33) also predicts that carrying one extra body-weight $M/m_{\text{body}} \approx 2$ may be done by a human supplying only half of the energy compared to a world-class cyclist ($e_{\text{h max}} \approx 4$ J/kg) while using a robot exoskeleton as efficient as the modern racing bicycle ($\eta \approx 0.95$).

VI. Discussion and Conclusion

Recently, a number of devices have been developed and used to reduce the metabolic cost of everyday tasks, with three distinct aims [35]–[37]: (i) reducing the metabolic energy cost of carrying extra load by reducing vertical oscillation of the center of mass, such as the "floating backpack" [38] inspired by bamboo poles [39], [40]; (ii) reducing the metabolic energy cost of carrying extra load by using energetically passive exoskeletons or rigid robot limbs to support the extra load instead of supporting the extra load by human muscles [41], [42]; and (iii) reducing the metabolic cost of carrying extra load using external energy provided by motors and batteries to assist the human with energetically active shoes [43]–[46], soft exosuits [47]–[49], as well as robot exoskeletons which provide appreciable weight support [50]–[52]. The combination of these approaches led us to study mechanically adaptive but energetically passive devices that inherit the defining aspects of bicycle mechanics.

In this work, we explored the theoretical limits of human-driven mechanically adaptive and energetically passive robot exoskeletons, the legged alternatives of the bicycle. We show that a 50% efficient exoskeleton enabling the human to supply the same amount of energy as the bicycle could accelerate one extra body weight up to the top race-walking speed in 10 steps (Fig. 2). Our finding assumes a spring legged exoskeleton where the spring is partly pre-compressed by the human before heel-strike, while the stiffness of the spring is changed at mid-stance (Fig. 1). We found the optimal feedback relation between the leg length and the leg stiffness could be implemented using a human-driven automaton (Section IV). We showed that the proposed optimal walking technique, defined by zero vertical velocities at heel-strike and toe-off, is not subject to walk-to-run transition limit predicted by the compass gait walking model (Section V-A). Finally, we showed that the limiting factors to increase the payload are (i) the maximum stiffness of the robot limbs, (ii) the maximum amount of energy supplied by the human per step, and (iii) the energy efficiency of the robot exoskeleton, instead of the energy storage, average force, and peak power capability of the human leg (Section V-F). Our results inform robot developers, designers, and control engineers of the theoretical limits of human-driven legged robots that could be used for transportation, sports, or emergency rescue.

While this paper thoroughly investigated the theoretical underpinnings of creating a legged exoskeleton for a fast-walking load-carrying task, a number of practical challenges in creating one such exoskeleton still remain to be elucidated. Most notably, the human-driven legged exoskeleton considered in this paper requires a special type of robot leg that could change its stiffness without affecting the energy stored by the spring [22], [53]. The function of such variable stiffness spring leg is twofold: first, it could enable the human to supply a large amount of energy by circumventing the force-velocity trade-off [54], [55] and configuration-dependent force limitations of the human limb [56]; and second, it could enable the robot limb to amplify the human leg force and power to support and accelerate a heavy load beyond the capability of the human limb alone. Research on developing spring legs that incorporate these novel features is underway [22].

Prior research has identified that swinging the legs is energetically expensive with extra weight added to the legs, as more torque is needed to accelerate and decelerate the legs [28], [57]–[59]. One way to mitigate the detrimental effect of added mass is by mechanically connecting the human arms to the robot legs, as shown in Fig. 1. In this way, the arms could help to provide the extra torque to swing the robot legs at the same frequency as the human legs. Another way to mitigate the aforementioned limitation is by using a hip spring [60], since swinging the legs is theoretically a zero-work task [30].

Prior research has also identified a number of challenges in interfacing robots with humans [59], [61]. One of these challenges is to provide a safe and comfortable interface where the force between the human and the robot is kept low [58], [62]. The same issue has been addressed in the bicycle using a seat and pedal, and a somewhat similar interface shown in Fig. 1, may be used between the human and a human-driven legged robot exoskeleton.

In addition to the above-mentioned practical issues, stability is also an important aspect of human-driven robot locomotion. We explored the local stability of the forward velocity in Section V-C, but stability of human-driven robot locomotion deserves further investigation. In this paper, the ability of the human to stably walk using the energetically passive exoskeleton was presumed, based on the ability of the human to choose a stable foot placement in each step [17], [63], [64], and based on the empirically established ability of humans to stably move with energetically passive devices, bicycles, ice-skates, and other similar devices. At the extreme of this spectrum is the pogo-stick which does not allow the human to make independent foot placement of the legs, but it still allows stable jumping. Stable walking is also feasible with motor-controlled adaptive but energetically passive prosthetic devices used by amputees to walk [65]. Based on these examples, we do not claim but conjecture that humans could learn a new gait, adapt to added mass, and use different sense of proprioception to achieve reliable terrine adaptation, as required to stably walk with a mechanically adaptive and energetically passive robot, similar to the conceptual robot shown in Fig. 1. We envision mechanically adaptive and energetically passive robots used for emergency rescue, sports, recreation, and transportation, as the legged alternative to the bicycle.

APPENDIX

A. Formulas in Section IV-A

The average velocity in the forward direction is defined by the step frequency and the step length $\bar{\dot{x}} = f l_s$. Using this relation, we approximate the ratio between the average velocity and the maximal average velocity with the ratio between the heel-strike velocity $\dot{x}_{\rm hs}$ and the maximal heel-strike velocity:

$$\frac{\bar{\dot{x}}}{\bar{\dot{x}}_{\max}} = \frac{f}{f_{\max}} \frac{l_s}{l_{s\max}} \approx \frac{\dot{x}_{\rm hs}}{\dot{x}_{\rm hs\max}}. \tag{34}$$

According to (34), the lower bound for the step length $l_{s\min}$ is obtained at the maximal step frequency $f = f_{\max}$:

$$\frac{l_{s\min}}{l_{s\max}} \approx \frac{\dot{x}_{\rm hs}}{\dot{x}_{\rm hs\max}}. \tag{35}$$

Using the inequality relation

$$l_{s\min} \le l_s \le l_{s\max}$$

together with $l_s = (l_0^2 - y_{\min}^2)^{\frac{1}{2}} + ((l_0 - \Delta l_{\rm hs})^2 - y_{\min}^2)^{\frac{1}{2}}$, $y_{\min}^2 - l_0^2 = \frac{1}{4} l_{s\max}^2$, (7), and (35), we derived (15) and (16).

B. Formulas in Section IV-B

The change of the momentum in the vertical direction will be zero if the vertical velocities are zero at toe-off and heel-strike:

$$M(\dot{y}_{\rm to} - \dot{y}_{\rm hs}) = 0 \approx \int_{x_{\rm hs}}^{x_{\rm to}} \left(F(x,y) \frac{y}{\sqrt{x^2+y^2}} - Mg \right) dx, \tag{36}$$

where x_{hs} and x_{to} denote the horizontal position of the center of mass at heel-strike and toe-off, $F(x, y)$ is the force exerted by the spring leg (2), and we assume $dx \approx \bar{\dot{x}}dt$.

We used $\forall t : y(t) = y_{\min}$, (36), and (7), to derive (18) and (19).

C. Formulas in Section IV-C

In order to compute the lower bound of the leg stiffness before mid-stance, we can derive the relation between the step frequency and the stiffness of the leg. Since the velocity of the center of mass is a bounded continuous function of the horizontal position x when considering just after heel-strike to toe-off, the mean value theorem for integrals implies:

$$\exists x^* \in [x_{\text{hs}}, x_{\text{to}}] : \frac{1}{(x_{\text{to}} - x_{\text{hs}})} \int_{x_{\text{hs}}}^{x_{\text{to}}} \dot{x}(x)dx = \bar{\dot{x}} = \dot{x}(x^*). \tag{37}$$

Consequently, using

$$l_s \leq l_{s\max} \quad \text{and} \quad f \leq f_{\max}, \tag{38}$$

we obtain the following relation:

$$\bar{\dot{x}}^2 = \dot{x}^2(x^*) = f^2 l_s^2 \leq f_{\max}^2 l_s^2, \tag{39}$$

where $\bar{\dot{x}}$ is the average top speed.

Subsequently, we define the horizontal velocity of the center of mass from mid-stance to toe-off:

$$\dot{x}_{\text{ms}}^2(x) = \dot{x}_{\text{to}}^2 + \frac{2}{M} \int_{x_{\text{ms}}}^{x_{\text{to}}} \left(F(x, y) \frac{x}{\sqrt{x^2 + y^2}} \right) dx. \tag{40}$$

Assuming $\forall t : y(t) = y_{\min}$, the integral in (40) can be evaluated, and x^* can be computed such that $\dot{x}_{\text{ms}}^2(x^*)$ defines the average top speed defined by the equality relation in (39):

$$\dot{x}_{\text{ms}}^2(x^*)|_{k_1 = k_2 = k_\infty, \Delta l_{\text{hs}} = 0} = f_{\max}^2 l_{s\max}^2. \tag{41}$$

Using (38) and (41), we obtain:

$$f_{\max}^2 l_s^2 \leq \dot{x}_{\text{ms}}^2(x^*). \tag{42}$$

Then, substituting (18) into (42), we derive

$$k_{1\min}(\Delta l_{\text{hs}}) \leq k_1. \tag{43}$$

Finally, we perform a Taylor series expansion of $k_{1\min}(\Delta l_{\text{hs}})$ with respect to Δl_{hs} at the top speed $\Delta l_{\text{hs}} \approx 0$, and find:

$$k_{1\min}(\Delta l_{\text{hs}}) = k_\infty - C(s_{\max}) \frac{\Delta l_{hs}}{l_0}, \tag{44}$$

where

$$C(s_{\max}) = \frac{2}{s_{\max}^2 \left(1 - \frac{1}{2} \left(\frac{1 - l^*}{(1 - \frac{1}{2}\sqrt{4 - s_{\max}^2})} \right)^2 \right)}, \tag{45}$$

and $l^* = (x^{*2} + y_{\min}^2)^{\frac{1}{2}} / l_0 \in [0, 1]$ is the average dimensionless leg length, computed using x^* as defined by (41). Using (43) and (44), we obtain (20) and (21).

REFERENCES

[1] G. A. Cavagna, F. P. Saibene, and R. Margaria, "Mechanical work in running," *J. Appl. Physiol.*, vol. 19, no. 2, pp. 249–256, Mar. 1964.

[2] S. Mochon and T. A. Mcmahon, "Ballistic walking," *J. Biomech.*, vol. 13, no. 1, pp. 49–57, Jan. 1980.

[3] G. M. O. Maloiy, N. C. Heglund, L. M. Prager, G. A. Cavagna, and C. R. Taylor, "Energetic cost of carrying loads: Have African women discovered an economic way?" *Nature*, vol. 319, no. 6055, pp. 668–669, Feb. 1986.

[4] A. E. Minetti, F. Formenti, and L. P. Ardigò, "Himalayan porter's specialization: Metabolic power, economy, efficiency and skill," *Proc. Roy. Soc. B, Biol. Sci.*, vol. 273, no. 1602, pp. 2791–2797, Nov. 2006.

[5] G. J. Bastien, P. A. Willems, B. Schepens, and N. C. Heglund, "The mechanics of head-supported load carriage by Nepalese porters," *J. Exp. Biol.*, vol. 219, no. 22, pp. 3626–3634, Nov. 2016.

[6] M. Foissac, G. Y. Millet, A. Geyssant, P. Freychat, and A. Belli, "Characterization of the mechanical properties of backpacks and their influence on the energetics of walking," *J. Biomech.*, vol. 42, no. 2, pp. 125–130, Jan. 2009.

[7] T. M. Griffin, T. J. Roberts, and R. Kram, "Metabolic cost of generating muscular force in human walking: Insights from load-carrying and speed experiments," *J. Appl. Physiol.*, vol. 95, no. 1, pp. 172–183, 2003.

[8] A. Grabowski, C. Farley, and R. Kram, "Independent metabolic costs of supporting body weight and accelerating body mass during walking," *J. Appl. Physiol.*, vol. 98, no. 2, pp. 579–583, 2005.

[9] D. P. Ferris, G. S. Sawicki, and M. A. Daley, "A physiologist's perspective on robotic exoskeletons for human locomotion," *Int. J. Humanoid Robot.*, vol. 4, no. 3, pp. 507–528, 2007.

[10] K. B. Pandolf, B. Givoni, and R. F. Goldman, "Predicting energy expenditure with loads while standing or walking very slowly," *J. Appl. Physiol.*, vol. 43, no. 4, pp. 577–581, Oct. 1977.

[11] T.-W. P. Huang and A. D. Kuo, "Mechanics and energetics of load carriage during human walking," *J. Exp. Biol.*, vol. 217, no. 4, pp. 605–613, 2014.

[12] J. M. Donelan, R. Kram, and A. D. Kuo, "Mechanical work for step-to-step transitions is a major determinant of the metabolic cost of human walking," *J. Exp. Biol.*, vol. 205, no. 23, pp. 3717–3727, Dec. 2002.

[13] A. Ruina, J. E. A. Bertram, and M. Srinivasan, "A collisional model of the energetic cost of support work qualitatively explains leg sequencing in walking and galloping, pseudo-elastic leg behavior in running and the walk-to-run transition," *J. Theor. Biol.*, vol. 237, no. 2, pp. 170–192, Nov. 2005.

[14] S. Dorel *et al.*, "Torque and power-velocity relationships in cycling: Relevance to track sprint performance in world-class cyclists," *Int. J. Sports Med.*, vol. 26, no. 9, pp. 739–746, Nov. 2005.

[15] A. D. Kuo, "Choosing your steps carefully," *IEEE Robot. Autom. Mag.*, vol. 14, no. 2, pp. 18–29, Jun. 2007.

[16] R. Alexander, "Walking and running: Legs and leg movements are subtly adapted to minimize the energy costs of locomotion," *Amer. Scientist*, vol. 72, no. 4, pp. 348–354, 1984.

[17] J. Pratt and R. Tedrake, "Velocity-based stability margins for fast bipedal walking," in *Fast Motions in Biomechanics and Robotics: Optimization and Feedback Control*, M. Diehl and K. Mombaur, Eds. Berlin, Germany: Springer, 2006, pp. 299–324.

[18] A. Sutrisno and D. J. Braun, "Enhancing mobility with quasi-passive variable stiffness exoskeletons," *IEEE Trans. Neural Syst. Rehabil. Eng.*, vol. 27, no. 3, pp. 487–496, Mar. 2019.

[19] A. Sutrisno and D. J. Braun, "How to run 50% faster without external energy," *Sci. Adv.*, vol. 6, no. 13, pp. 1–11, Mar. 2020.

[20] D. J. Braun, S. Apte, O. Adiyatov, A. Dahiya, and N. Hogan, "Compliant actuation for energy efficient impedance modulation," in *Proc. IEEE Int. Conf. Robot. Autom. (ICRA)*, May 2016, pp. 636–641.

[21] D. J. Braun, V. Chalvet, T.-H. Chong, S. S. Apte, and N. Hogan, "Variable stiffness Spring actuators for low-energy-cost human augmentation," *IEEE Trans. Robot.*, vol. 35, no. 6, pp. 1435–1449, Dec. 2019.

[22] T. Zhang and D. J. Braun, "Human driven compliant transmission mechanism," in *Proc. IEEE Int. Conf. Robot. Autom. (ICRA)*, May 2021, pp. 7094–7099.

[23] P. Holmes, R. J. Full, D. Koditschek, and J. Gückenheimer, "The dynamic of legged locomotion: Model, analyses, and challenges," *SIAM Review*, vol. 48, no. 2, pp. 207–304, 2006.

[24] M. Garcia, A. Chatterjee, A. Ruina, and M. Coleman, "The simplest walking model: Stability, complexity, and scaling," *ASME J. Biomech. Eng.*, vol. 120, no. 2, pp. 281–288, 1998.

[25] S. H. Hyon and T. Emura, "Energy-preserving control of a passive one-legged running robot," *Adv. Robot.*, vol. 18, no. 4, pp. 357–381, Jan. 2004.

[26] A. Minetti, J. Pinkerton, and P. Zamparo, "From bipedalism to bicyclism: Evolution in energetics and biomechanics of historic bicycles," *Proc. Roy. Soc. London B, Biol. Sci.*, vol. 268, pp. 1351–1360, Aug. 2001.

[27] B. Hanley, A. Bissas, and A. Drake, "Kinematic characteristics of elite men's and women's 20 km race walking and their variation during the race," *Sports Biomech.*, vol. 10, no. 2, pp. 110–124, Jun. 2011.

[28] R. C. Browning, J. R. Modica, R. Kram, and A. Goswami, "The effects of adding mass to the legs on the energetics and biomechanics of walking," *Med. Sci. Sports Exerc.*, vol. 39, no. 3, pp. 515–525, Mar. 2007.

[29] D. A. Raichlen, H. Pontzer, and L. J. Shapiro, "A new look at the dynamic similarity hypothesis: The importance of swing phase," *Biol. Open*, vol. 2, no. 10, pp. 1032–1036, Oct. 2013.

[30] A. D. Kuo, "Energetics of actively powered locomotion using the simplest walking model," *ASME J. Biomech. Eng.*, vol. 124, no. 1, pp. 113–120, Mar. 2002.

[31] A. Sørensen, T. K. Aune, V. Rangul, and T. Dalen, "The validity of functional threshold power and maximal oxygen uptake for cycling performance in moderately trained cyclists," *Sports*, vol. 7, no. 10, p. 217, Oct. 2019.

[32] E. Buckingham, "On physically similar systems; illustrations of the use of dimensional equations," *Phys. Rev.*, vol. 4, no. 4, pp. 345–376, Oct. 1914.

[33] G. A. Cavagna and M. Kaneko, "Mechanical work and efficiency in level walking and running," *J. Physiol.*, vol. 268, no. 2, pp. 467–481, 1977.

[34] M. Srinivasan and A. Ruina, "Computer optimization of a minimal biped model discovers walking and running," *Nature*, vol. 439, pp. 72–75, Sep. 2006.

[35] A. M. Dollar and H. Herr, "Lower extremity exoskeletons and active orthoses: Challenges and state-of-the-art," *IEEE Trans. Robot.*, vol. 24, no. 1, pp. 144–158, Feb. 2008.

[36] A. J. Young and D. P. Ferris, "State of the art and future directions for lower limb robotic exoskeletons," *IEEE Trans. Neural Syst. Rehabil. Eng.*, vol. 25, no. 2, pp. 171–182, Feb. 2017.

[37] G. S. Sawicki, O. N. Beck, I. Kang, and A. J. Young, "The exoskeleton expansion: Improving walking and running economy," *J. Neuroeng. Rehabil.*, vol. 17, no. 1, pp. 1–9, Dec. 2020.

[38] L. C. Rome, L. Flynn, and T. D. Yoo, "Rubber bands reduce the cost of carrying loads," *Nature*, vol. 444, no. 7122, pp. 1023–1024, 2006.

[39] R. T. Schroeder, J. L. Croft, G. D. Ngo, and J. E. A. Bertram, "Properties of traditional bamboo carrying poles have implications for user interactions," *PLoS ONE*, vol. 13, no. 5, May 2018, Art. no. e0196208.

[40] R. T. Schroeder, J. E. A. Bertram, V. S. Nguyen, V. V. Hac, and J. L. Croft, "Load carrying with flexible bamboo poles: Optimization of a coupled oscillator system," *J. Exp. Biol.*, vol. 222, no. 23, Dec. 2019, Art. no. jeb203760.

[41] C. Walsh, K. Pasch, and H. Herr, "An autonomous, underactuated exoskeleton for load-carrying augmentation," in *Proc. IEEE/RSJ Int. Conf. Intell. Robots Syst.*, Oct. 2006, pp. 1410–1415.

[42] C. Weiss. *Have Your Chair and Sit in it too—Revisiting the Wearable Chairless Chair*. News Atlas. Accessed: Jan. 12, 2022. [Online]. Available: https://newatlas.com/wearable-chairless-chair-2018/53521/

[43] L. M. Mooney, E. J. Rouse, and H. M. Herr, "Autonomous exoskeleton reduces metabolic cost of walking," in *Proc. 36th Annu. Int. Conf. IEEE Eng. Med. Biol. Soc.*, Aug. 2014, pp. 3065–3068.

[44] J. Chung, R. Heimgartner, C. T. Oneill, N. S. Phipps, and C. J. Walsh, "Exoboot, a soft inflatable robotic boot to assist ankle during walking: Design, characterization and preliminary tests," in *Proc. 7th IEEE Int. Conf. Biomed. Robot. Biomechtronics (Biorob)*, Aug. 2018, pp. 509–516.

[45] M. K. MacLean and D. P. Ferris, "Energetics of walking with a robotic knee exoskeleton," *J. Appl. Biomech.*, vol. 35, no. 5, pp. 320–326, Oct. 2019.

[46] K. A. Witte, P. Fiers, A. L. Sheets-Singer, and S. H. Collins, "Improving the energy economy of human running with powered and unpowered ankle exoskeleton assistance," *Sci. Robot.*, vol. 5, no. 40, Mar. 2020, Art. no. eaay9108.

[47] F. A. Panizzolo *et al.*, "A biologically-inspired multi-joint soft exosuit that can reduce the energy cost of loaded walking," *J. Neuroeng. Rehabil.*, vol. 13, no. 1, pp. 1–14, Dec. 2016.

[48] J. Kim *et al.*, "Reducing the metabolic rate of walking and running with a versatile, portable exosuit," *Science*, vol. 365, no. 6454, pp. 668–672, 2019.

[49] M. Xiloyannis *et al.*, "Soft robotic suits: State of the art, core technologies, and open challenges," *IEEE Trans. Robot.*, vol. 38, no. 3, pp. 1–20, Jun. 2021.

[50] A. Zoss, H. Kazerooni, and A. Chu, "On the mechanical design of the Berkeley lower extremity exoskeleton (BLEEX)," in *Proc. IEEE/RSJ Int. Conf. Intell. Robots Syst.*, Aug. 2005, pp. 3465–3472.

[51] Y. Sankai, "Hal: Hybrid assistive limb based on cybernics," in *Robotics Research*, M. Kaneko and Y. Nakamura, Eds. Berlin, Germany: Springer, 2011, pp. 25–34.

[52] W. Kim, H. Lee, D. Kim, J. Han, and C. Han, "Mechanical design of the Hanyang exoskeleton assistive robot(HEXAR)," in *Proc. 14th Int. Conf. Control, Autom. Syst. (ICCAS)*, Oct. 2014, pp. 479–484.

[53] S. Y. Kim and D. J. Braun, "Novel variable stiffness Spring mechanism: Modulating stiffness independent of the energy stored by the Spring," in *Proc. IEEE/RSJ Int. Conf. Intell. Robots Syst. (IROS)*, Sep. 2021, pp. 8232–8237.

[54] A. V. Hill, "The maximum work and mechanical efficiency of human muscles, and their most economical speed," *J. Physiol.*, vol. 56, nos. 1–2, pp. 19–41, Feb. 1922.

[55] M. Ilton *et al.*, "The principles of cascading power limits in small, fast biological and engineered systems," *Science*, vol. 360, no. 6387, Apr. 2018, Art. no. eaao1082.

[56] E. Ofori, J. Shim, and J. J. Sosnoff, "The influence of lower leg configurations on muscle force variability," *J. Biomech.*, vol. 71, pp. 111–118, Apr. 2018.

[57] J. Doke, J. M. Donelan, and A. D. Kuo, "Mechanics and energetics of swinging the human leg," *J. Exp. Biol.*, vol. 208, no. 3, pp. 439–445, 2005.

[58] M. S. Cherry, S. Kota, and A. Young, "Running with an elastic lower limb exoskeleton," *J. Appl. Biomech.*, vol. 32, no. 3, pp. 269–277, 2016.

[59] D. P. Ferris and W. S. Barrutia, "Novel designs for passive elastic lower limb exoskeletons," in *Wearable Robotics: Challenges and Trends*, J. C. Moreno, J. Masood, U. Schneider, C. Maufroy, and J. L. Pons, Eds. Cham, Switzerland: Springer, 2022, pp. 27–31.

[60] C. W. Mathews and D. J. Braun, "Parallel variable stiffness actuators," in *Proc. IEEE/RSJ Int. Conf. Intell. Robots Syst. (IROS)*, Sep. 2021, pp. 8225–8231.

[61] G. Elliott, A. Marecki, and H. Herr, "Design of a Clutch–Spring knee exoskeleton for running," *J. Med. Devices*, vol. 8, no. 3, Sep. 2014.

[62] M. B. Yandell, B. T. Quinlivan, D. Popov, C. Walsh, and K. E. Zelik, "Physical interface dynamics alter how robotic exosuits augment human movement: Implications for optimizing wearable assistive devices," *J. Neuroeng. Rehabil.*, vol. 14, no. 1, pp. 1–11, Dec. 2017.

[63] T. Koolen, T. de Boer, J. Rebula, A. Goswami, and J. Pratt, "Capturability-based analysis and control of legged locomotion, Part 1: Theory and application to three simple gait models," *Int. J. Robot. Res.*, vol. 31, no. 9, pp. 1094–1113, 2012.

[64] P. Zaytsev, W. Wolfslag, and A. Ruina, "The boundaries of walking stability: Viability and controllability of simple models," *IEEE Trans. Robot.*, vol. 34, no. 2, pp. 336–352, Apr. 2018.

[65] B. E. Lawson, B. Ruhe, A. Shultz, and M. Goldfarb, "A powered prosthetic intervention for bilateral transfemoral amputees," *IEEE Trans. Biomed. Eng.*, vol. 62, no. 4, pp. 1042–1050, Apr. 2015.